Studies on Binary and Ternary Blends of Polypropylene with SEBS, PS, and HDPE. I. Melt Rheological Behavior

A. K. GUPTA and S. N. PURWAR, *Centre for Materials Science and Technology, Indian Institute of Technology, New Delhi 110 016, India*

Synopsis

Studies are reported on melt rheological behavior of some binary and ternary blends of polypropylene (PP) with one or two of the following polymers: styrene–*b*-ethylene butylene–*b*-styrene triblock copolymer (SEBS), polystyrene (PS), and high-density polyethylene (HDPE). Blend composition of the binary blends PP/*X* or ternary blends PP/*X*/*Y* were so chosen that the former represent addition of 10 wt % *X* to PP while the latter represent 10 wt % addition of *X* or *Y* to the PP/*Y* or PP/*X* blend of constant composition 90:10 by weight, *X*/*Y* being SEBS, PS, or HDPE. Measurements were made on a capillary rheometer using both temperature elevation and constant temperature methods to study the behaviors prior to flow and in the flow region. Flow behavior, measured at a constant temperature (200°C) and varying shear stress (from 1.0 to 5.0 $\times$ 10^6 dyn/cm^2) to evaluate melt viscosity and melt elasticity parameters, is discussed for its dependence on the nature of the blend. Extrudate distortion, studied as a function of shear stress to evaluate the critical shear stress for the onset of extrudate distortion, showed differences in the tendency for extrudate distortion or melt fracture of these different blends. Also discussed is the effect of melt viscosity and melt elasticity on extrudate distortion behavior at the critical condition, which showed a unique critical value of the ratio (melt elasticity parameter)$^{1/2}$/(melt viscosity) for all these blends. Blend morphologies before and after the flow through the capillary are investigated through scanning electron microscopy, and their correlations with rheological parameters of the melt are discussed.

INTRODUCTION

Studies on the blends of polypropylene (PP) with a recently commercialized thermoplastic elastomer, viz., styrene–*b*-ethylene-co-butylene–*b*-styrene triblock copolymer (SEBS), have been the subject of our previous publications.[1–3] The effect of blend composition on the melt rheology,[1] tensile yield behavior,[3] impact strength,[1] and crystallization of PP component and its effect on tensile properties[2] of PP/SEBS blend have shown many desirable improvements in their properties. Though the improvement in impact strength was greater at higher SEBS contents, the tensile properties showed some deterioration at such compositions. Melt flow behavior showed some optimum improvements, desirable from the point of view of processability, around the blend composition with 5–10 wt % SEBS content. This suggests a greater scope of the applicability of PP and emphasizes the need for selection of suitable blend composition for the necessary compromise of various properties desirable for any specific end-use application.

Journal of Applied Polymer Science, Vol. 30, 1777–1798 (1985)
 CCC 0021-8995/85/051777-22$04.00

Some recent studies involving SEBS, reported by Paul et al.,[4,5] Sperling et al.,[6,7] and Yee and Diamant[8] are devoted to: (i) the blends of SEBS with polystyrene (PS),[8] polyethylene terephthalate (PET)/high-density polyethylene (HDPE) blend,[5] and PS/HDPE blend[4]; (ii) the preparation of thermoplastic interpenetrating networks involving SEBS and the random copolymer of methacrylic acid, isoprene and styrene[6]; and (iii) electron beam induced crosslinking of SEBS.[7] Among the several interesting findings of these studies are the improvements in ductility, compatibilization of the components of immiscible polymer blends, and some improvements in melt rheological properties, etc.

In this paper we present a study on the ternary blends PP/SEBS/PS and PP/SEBS/HDPE with blend composition so chosen that the major component of the blend is PP, which is 80% by weight of the blend, and the remaining 20% of the blend comprised of two components—one SEBS and the other PS or HDPE—in equal proportion. This choice of the blend composition has the advantage that the blends may be seen either (i) to represent the effect of 10 wt % addition of SEBS to the PP/PS and PP/HDPE binary blends or (ii) to represent the effect of 10 wt % addition of PS or HDPE to the PP/SEBS blend, at identical blending ratio (i.e., approximately 90% PP and 10% of the other component) of each of these three reference binary blend systems. In addition to the ternary blends, the corresponding binary blends PP/SEBS, PP/PS, and PP/HDPE prepared under similar conditions are also investigated. Results on these binary blends provide not only some useful informations about these blends but also serve as useful reference for ascertaining the origins of the behaviors observed for the respective ternary blends.

Studies presented include: (i) melt rheological properties measured on a capillary rheometer following both (a) temperature elevation and (b) constant temperature procedures, to study the behavior at temperatures prior to flow and the melt viscosity and melt elasticity in the flow region; (ii) melt fracture or extrudate distortion studied at constant length/radius (L/R) ratio of the capillary at varying shear stress; (iii) morphology and state of dispersion by scanning electron microscopy; and (iv) differential scanning calorimetric studies for melting behavior of PP component in the various blends.

EXPERIMENTAL

Materials

Polymers used in the present study were the commercially available products of moulding grades: (i) isotactic polypropylene (PP): Koylene M 3030 melt flow index 3.0, of Indian Petro-chemicals Corporation Ltd.; (ii) high-density polyethylene (HDPE): Hostalene GD-7250, melt flow index 1.7; (iii) polystyrene (PS): grade HCG 100 of Hindustan Polymers Ldt.; and (iv) Styrene–*b*-ethylene-co-butylene–*b*-styrene block copolymer (SEBS): Kraton G 1652 of Shell Chemical Company. The most commonly stated[4,6,7] molecular description of this latter sample (i.e., SEBS) is that it is a triblock copolymer with the central block of hydrogenated polybutadiene (molecular wt $\simeq$39

$\times 10^3$) flanked at both ends by polystyrene blocks (molecular wt $\simeq 8 \times 10^3$), with weight fraction of styrene units $\simeq$30%. Some additional details, such as the overall weight average and number average molecular weights and the ratio of ethylene and butylene units (E/B) in the EB block, found by Kratochvil[9] are as follows: $M_w = 60 \times 10^3$, $M_n = 53 \times 10^3$, and E/B = 0.52.

Preparation of Blends

All the binary and ternary blends were prepared by melt blending in a single screw extruder Betol BM 1820 under identical conditions of the experiment in all cases, using screw speed 40 rpm and temperature profile 200°C, 210°C, 220°C, and 200°C at the first, second, third, and the die zones, respectively. Blend compositions of the various samples and their nomenclature are shown in Table I. Blends received from the extruder in the form of thick filaments were cut into small pellets, washed, and dried. For some scanning electron microscopic studies, compression-molded sheets were prepared on a Carver Laboratory Press at 220°C and 5000 psi pressure, which were fractured manually by cooling in liquid air.

Measurement of Rheological Properties

Melt rheological measurements were made on a piston type capillary rheometer, Koka Flow Tester of Schimadzu Seisakusho Ltd., Japan, using dies of circular cross section, length to radius (L/R) ratios 4 and 10, and flat at the entrance region. Measurements were carried out using both the standard procedures,[10] viz., (i) the temperature elevation method to obtain "plasticity curves" and (ii) the fixed temperature method to obtain "flow curves," using constant pressure (or shear stress) for (i) and variable pressure (or shear stress) for (ii). Some additional details of these experiments would appear with the description of the results in a subsequent section.

Scanning Electron Microscopy

Scanning electron micrographs of fracture surfaces of compression-molded sheets and capillary rheometer extrudates, fractured manually after cooling in liquid air, were recorded on a Stereoscan S4-10 of Cambridge

TABLE I
Nomenclature and Compositions of the Various Samples

	Composition (wt %)			
Sample designation	PP	SEBS	PS	HDPE
PP	100	—	—	—
PP/SEBS	90	10	—	—
PP/PS	90	—	10	—
PP/HDPE	90	—	—	10
PP/SEBS/PS	80	10	10	—
PP/SEBS/HDPE	80	10	—	10

Scientific Instruments, Ltd. Samples were etched in xylene at room temperature to dissolve out the SEBS and PS phases.

RESULTS AND DISCUSSION

Plasticity Curves

Plasticity curves showing the plunger displacement as function of temperature (or time) in the region prior to flow and after flow are shown in Figure 1, in the form as recorded under identical conditions for the various samples. The different regions of plasticity curves are described[10] as follows: (i) the region AB of downward movement of plunger is due to compaction of polymer chips during softening; temperature at B is denoted as softening point T_s; (ii) the region BD is the melting region where the upward movement of the plunger is due to melt elasticity and volume expansion on crystallite melting; the temperature at midpoint C of region BD is denoted

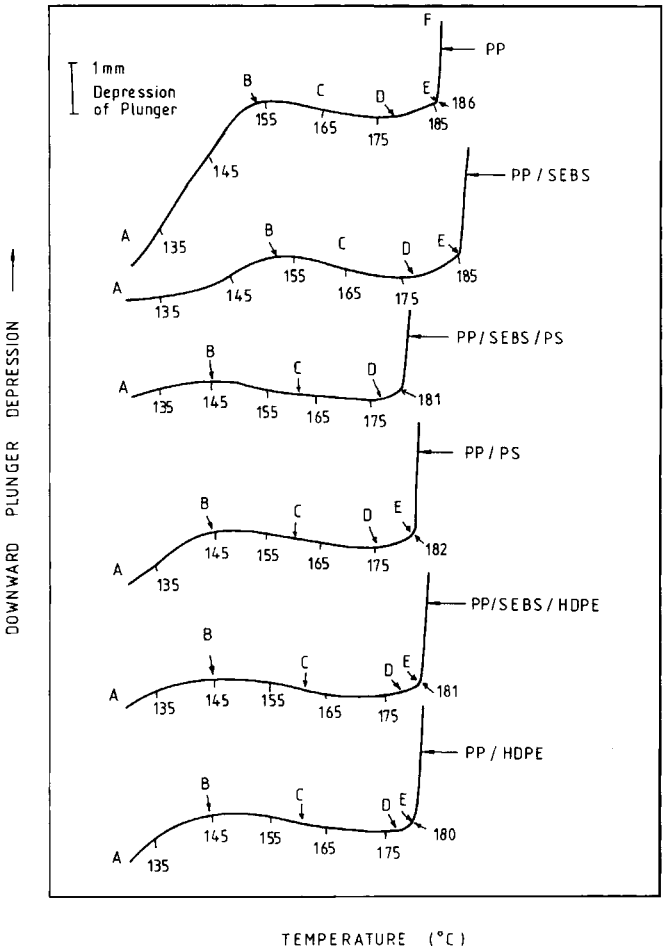

Fig. 1. Plasticity curves of the various samples recorded at $\Delta P = 30$ kg/cm^2 and die L/R ratio 4.

as melting point T_m; (iii) beyond point D flow through capillary orifice starts, and occurs at slower rate in region DE and at faster rate in region EF; temperatures at points D and E are denoted as "initial" and "final" flows temperatures T_{f1} and T_{f2}, respectively.

Values of T_s, T_m, T_{f1}, and T_{f2}, given in Table II, show distinctly lower values for the blends than PP; however, the differences are less distinct in case of T_{f1}. Although the lowering of softening, melting, and flow temperatures are advantageous from the point of view of processing behavior, the decrease for the present blend compositions are only by 5–10°C. It is, however, remarkable that decrease in these processing parameters is much smaller in PP/SEBS than the other blends, thus indicating the advantages of going in for these ternary blends. Thus the advantages of incorporation of SEBS to PP can be obtained along with some cost reduction on incorporation of the third component HDPE or PS without loss of ease of processability.

Differences in the rates of increase of temperature of the different samples is also apparent from these plasticity curves which were recorded using constant sample weight and constant rate of power supplied to the heater. The time $t_{175-135}$ taken for a constant temperature rise from 135°C to 175°C, shown in Table II, illustrates this difference in rate of temperature rise of these samples. This seems due to the differences of specific heats arising from the relative predominence of the endothermic (i.e., crystallite melting of PP and HDPE) and exothermic (i.e., crystallization of PP and HDPE) transitions occurring in these blends in this temperature region.[2,11]

The DSC melting endotherms of PP in these various samples, presented in Figure 2, show the temperatures of the melting peak (T_p) given in the last column of Table II. Closeness of T_p with T_m for unblended PP is noteworthy, whereas for the blends T_m values are only slightly lower than T_p. It may thus be stated that the T_m determined from the plasticity curve is quite consistent with the crystallite melting peak temperature for the single-component system, or of the crystallizable major component in the binary or ternary blends.

Shear Stress–Shear Rate Curves

Volumetric flow rate measurements at various pressures at a constant temperature (200°C) were used to calculate shear stress $(\tau_w)_{app}$, the apparent

TABLE II
Softening (T_s), Melting (T_m), Initial and Final Flow (T_{f1} and T_{f2}) Temperatures, and Time for Constant Temperature Rise 135–175°C ($t_{175-135}$)

Sample	T_s (°C)	T_m (°C)	T_{f1} (°C)	T_{f2} (°C)	$t_{175-135}$ (s)	T_p (°C)
PP	154	165	178	186	249	166.2
PP/SEBS	150	164	177	185	276	165.8
PP/PS	145	160	175	182	249	165.5
PP/HDPE	145	160	176	180	268	165.4
PP/SEBS/PS	138	161	176	181	238	165.4
PP/SEBS/HDPE	142	161	177	181	261	165.7

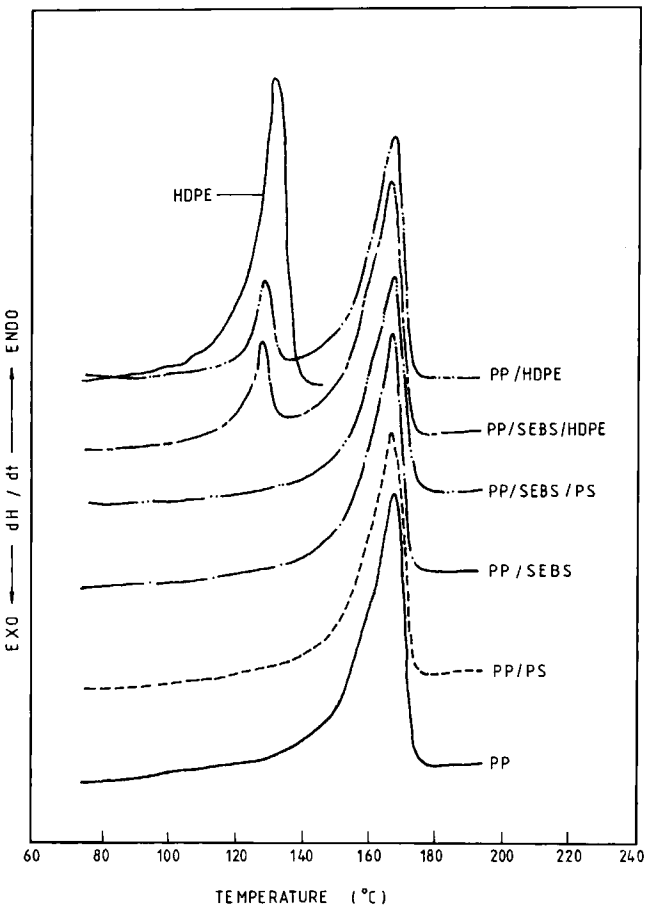

Fig. 2. DSC thermograms in the melting region of PP.

shear stress at the wall and shear rate ($\dot{\gamma}$) according to the following expressions[12]:

$$(\tau_w)_{app} = \Delta P/2(L/R) \tag{1}$$

$$\dot{\gamma} = 4Q/\pi R^3 \tag{2}$$

where ΔP is the pressure difference between the entrance and exit of the capillary. L/R is the length/radius ratio (which was equal to 10 for the capillary die used). Q is the volumetric flow rate (cm^3/s) and R is the radius of the capillary (cm).

Shear stress versus shear rate curves for these samples are presented in Figure 3. These curves are sufficiently linear over the entire range of these measurements, implying the validity of the power law relationship[12] of the following type:

$$(\tau_w)_{app} = K\dot{\gamma}^n \tag{3}$$

with values of n and K shown in Table III. These values of n, viz., between

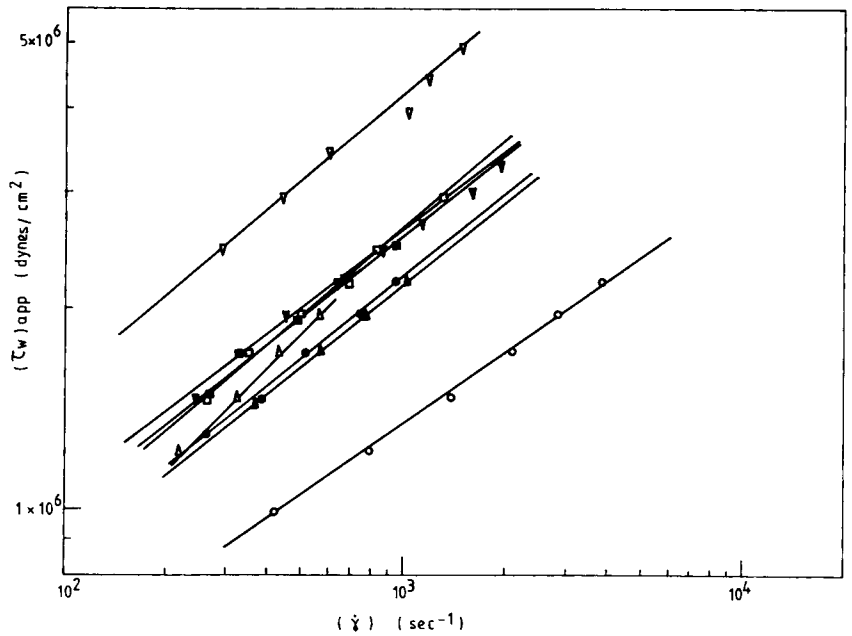

Fig. 3. Variation of shear stress vs. shear rate: (○) PP; (△) PS; (▽) HDPE; (□) PP/SEBS; (●) PP/PS; (▲) PP/HDPE; (▼) PP/SEBS/HDPE. (■) PP/SEBS/PS.

0.38 and 0.49, being lower than unity, indicate the pseudoplastic nature[13] of the melts of all these samples. These values of n are of comparable magnitude with those reported for other single-phase or two-phase polymeric systems such as HDPE (0.31–0.427)[14] LDPE (0.398),[14] HIPS (0.288, 0.297),[15] and ABS (0.378).[15] The differences in the values of n for the various samples shown in Table III may imply the differences in the ease of flow in these samples, but no definite comment about their origin is possible from these data alone.

TABLE III
Values of Exponent n of Eq. (3), Measured η_{app} and $(\eta_{app})_{blend}$ Calculated from Log-Addivity Rule

Sample	$\eta_{app} \times 10^{-3}$ (P)		Calculated $(\eta_{app})_{blend} \times 10^{-3}$ (P)[b]	n
	a	b		
PP	1.05	0.68	—	0.38
SEBS	—	60.0	—	—
PS	4.51	3.5	—	—
HDPE	—	12.0	—	—
PP/SEBS	5.47	3.94	1.064	0.44
PP/PS	3.84	2.61	0.801	0.49
PP/HDPE	3.92	2.56	0.906	0.41
PP/SEBS/PS	5.47	3.94	1.254	0.41
PP/SEBS/HDPE	5.92	4.30	1.418	0.42

[a] At shear stress 1.47×10^6 dyn/cm².
[b] At shear stress 1.96×10^6 dyn/cm².

Melt Viscosity

Apparent melt viscosity η_{app} (called hereafter melt viscosity) is calculated from these data according to the following expression:

$$\eta_{app} = (\tau_w)_{app}/\dot{\gamma} \tag{4}$$

Variation of melt viscosity with shear stress and shear rate are shown in Figures 4 and 5. The decrease of melt viscosity with increasing shear stress or shear rate is quite linear over the entire range of measurements obeying the following power law relationship[12]:

$$\eta_{app} = K^{1/n}(\tau_w)_{app}^{(n-1)/n} = K\dot{\gamma}^{n-1} \tag{5}$$

with values of n consistent with those shown in Table II for the respective blends. Slopes of these curves for the various samples differ quite insignificantly as apparent also from the small differences in the values of n.

Values of η_{app} at constant shear stress are presented in Table III for illustrating the effect of the nature of blend on melt viscosity. Though the melt viscosities of the individual components of these blends differ widely, the viscosities of all these binary or ternary blends do not differ greatly. Among the binary blends, PP/PS and PP/HDPE have slightly lower viscosity than the PP/SEBS blend, implying some role of SEBS in increasing the melt viscosity. The melt viscosity of the ternary blends PP/SEBS/PS and PP/SEBS/HDPE is higher than that of the binary blends PP/PS and

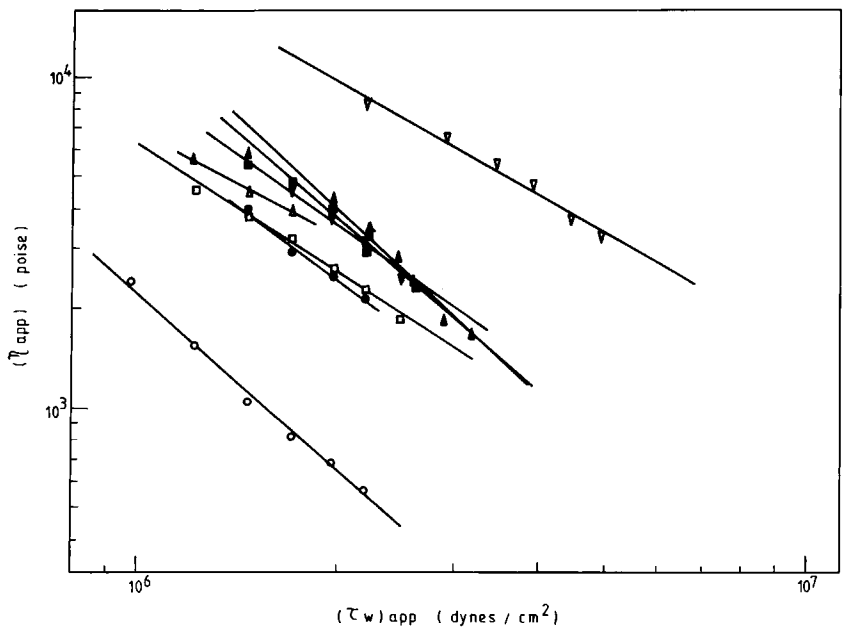

Fig. 4. Variation of apparent melt viscosity η_{app} with shear stress: (○) PP; (△) PS; (▽) HDPE; (□) PP/SEBS; (●) PP/PS; (▲) PP/HDPE; (▼) PP/SEBS/HDPE; (■) PP/SEBS/PS.

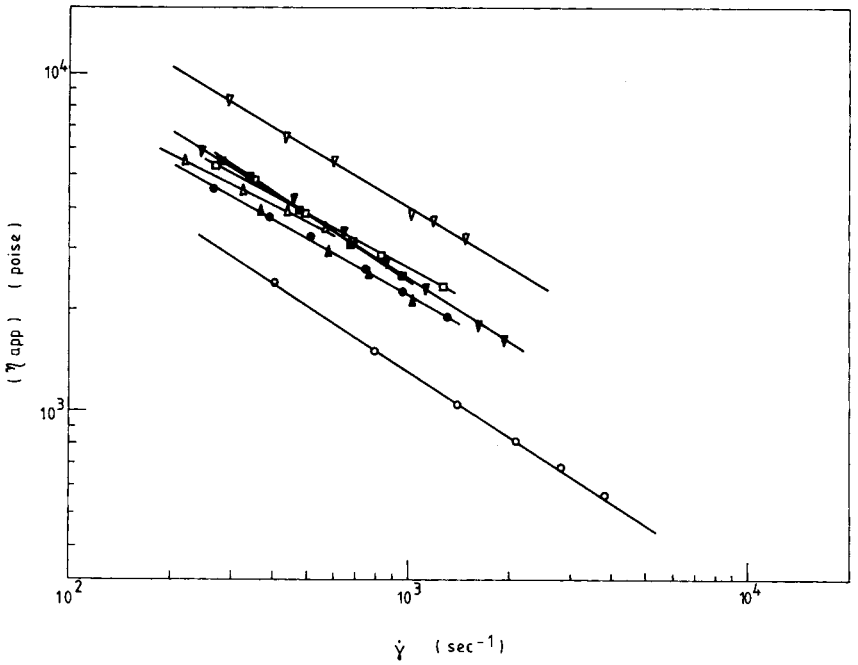

Fig. 5. Variation of apparent melt viscosity η_{app} with shear rate: (○) PP; (△) PS; (▽) HDPE; (□) PP/SEBS; (●) PP/PS; (▲) PP/HDPE; (▼) PP/SEBS/HDPE; (■) PP/SEBS/PS.

PP/HDPE but comparable to that of the binary blend PP/SEBS. Since the SEBS content was the same (i.e., 10 wt %) in all these three SEBS containing blends, it is astonishing to note that SEBS has greater tendency to increase the melt viscosity of PP than of these PP/PS and PP/HDPE blends. This suggests that the incorporation of SEBS as a third component in the binary blends PP/PS and PP/HDPE, if desirable from the point of view of other properties,[5] does not adversely affect the melt viscosity properties.

In a recent review of melt flow behavior of polymer blends, Utracki[16] showed that the positive or negative deviation of measured viscosity from that calculated from log-additivity rule [such as, for example, eq. (6)] is indicative of strong or weak interactions between the phases of the blend.

$$\ln(\eta_{app})_{blend} = \sum_i w_i \ln(\eta_{app})_i \tag{6}$$

where w_i is weight fraction of the ith component of the blend. As shown in Table III, the measured melt viscosity is higher than $(\eta_{app})_{blend}$ calculated by the log-additivity rule [eq. (6)], indicating positive deviation blend (PDB) character of all these blends. According to Utracki,[16] immiscible blends show negative deviation, while the positive deviation is expected for miscible liquids with high solubility and homologous polymer blends. The observed PDB behavior of the present immiscible blends seems to imply the contribution of not only the interphase interactions but also of the viscosity difference of the matrix and the suspensions. The suspensions in these blends have much higher viscosity than the matrix, and even the small

weight fraction (i.e., 10%) of the suspensions produces considerable increase in viscosity.

Melt Elasticity

A property of non-Newtonian viscoelastic fluids important in the choice of their processing parameters is their melt elasticity behavior, which causes the expansion of the fluid upon exiting from the die, also known as the die swell. Such an effect arises due to the recovery of the elastic deformation imposed in the capillary.[12,17-20] The die-swell ratio D_i/D, where D_i and D are, respectively, the diameters of extrudate and die, was determined at various shear stresses for these samples. Various other parameters characterizing melt elasticity, viz., the first normal stress difference $(\tau_{11} - \tau_{22})$, recoverable shear strain (γ_R), and the apparent shear modulus (G), were evaluated from these data according to following relations[12] using Tanner's expression[21] for $(\tau_{11} - \tau_{22})$ based on assumption of elastic Hookes law behaviour in shear:

$$(\tau_{11} - \tau_{22}) = 2\tau_w[2(D_i/D)^6 - 2]^{1/2} \tag{7}$$

$$\gamma_R = (\tau_{11} - \tau_{22})/2\tau_w \tag{8}$$

$$G = \tau_w/\gamma_R \tag{9}$$

Values of these parameters at constant shear stress are shown in Table IV. Higher values of $(\tau_{11} - \tau_{22})$, γ_R, or D_i/D and lower values of G imply greater elastic recoverability, hereafter referred as the higher melt elasticity in the subsequent discussion. The blends containing SEBS, viz., PP/SEBS, PP/SEBS/PS, and PP/SEBS/HDPE blends show lower melt elasticity than PP or the PP/PS and PP/HDPE blends. This suggests a significant role of the SEBS elastomer in the reduction of melt elasticity. The same 10 wt % addition of SEBS produces greater reduction of melt elasticity in the PP/PS and PP/HDPE blends than the unblended PP. Among the two ternary blends, the PP/SEBS/HDPE has lower melt elasticity than the PP/SEBS/PS blend.

TABLE IV
Values of the Various Melt Elasticity Parameters at a Constant Shear Stress 1.96×10^6 dyn/cm²

Sample	D_i/D	$(\tau_{11} - \tau_{22})$ $\times 10^{-6}$ (dyn/cm²)	γ_R	$\times 10^{-6G}$ (dyn/cm²)
PP	2.18	57.2	14.6	0.130
PP/SEBS	1.94	40.1	10.2	0.197
PP/PS	2.50	86.5	22.0	0.088
PP/HDPE	2.48	84.4	21.0	0.091
PP/SEBS/PS	1.78	28.7	7.3	0.268
PP/SEBS/HDPE	1.58	21.2	5.4	0.363

In addition to its effect on the die swell, the melt elasticity influences also the melt fracture or the extrudate distortion, as will be discussed in the subsequent section.

Extrudate Distortion

The melt fracture or extrudate distortion behavior, which is important in polymer processing to achieve acceptable product quality, is studied for these blends at various extrusion pressures ΔP (varying in the steps of 5 kg/cm^2) and at a constant L/R ratio of the die. The critical value of the pressure ΔP_{crit}, (or shear stress), at which the extrudate distortion first appears is determined to distinguish these blends for their tendencies for extrudate distortion. We have also examined the effect of melt flow parameters (melt viscosity and melt elasticity) at the critical shear stress on the tendency for extrudate distortion of these samples.

Photographs of the extrudates, shown in Figure 6, illustrate the effect of increasing pressure (or shear stress) on the distortion of extrudate surface. At lower shear stresses the extrudate surface is quite smooth in all these samples, while at higher shear stresses the extrudate distortion is apparent in all the samples except the HDPE. In other words, the severity of extrudate distortion increases with increasing shear stress. Thus an attempt to check the extrudate distortion by lowering the shear stress would be accompanied by a lowering of the flow rate and thus have its bearing on the production rate in the polymer processing industry. As will be described below, this study shows that the extrudate distortion can be reduced by blending without adversely affecting the flow rate.

Values of ΔP_{crit} for the various samples are shown in Table V; HDPE, however, showed no distortion of extrudate up to the highest limit of these measurements, i.e., 110 kg/cm^2. Since a higher value of ΔP_{crit} indicates a lower tendency for extrudate distortion, the following inferences are possible from these results:

1. PP and the binary blend PP/PS have the highest tendency for extrudate distortion, showing equal values of $\Delta P_{crit} = 35$ kg/cm^2; further distinction of these two samples would be possible from additional experiments using a smaller step of variation of ΔP.
2. Addition of 10 wt % SEBS reduces the tendency for extrudate distortion in PP as well as the PP/PS and PP/HDPE blends.
3. HDPE is more effective in reducing tendency for extrudate distortion than PS, as apparent from a comparison of ΔP_{crit} values for PP/HDPE and PP/PS blends.
4. Among the ternary blends, PP/SEBS/HDPE has a lower tendency for extrudate distortion than PP/SEBS/PS, which further supports the greater effect of HDPE on extrudate distortion than PS, as stated in 3 above.
5. By comparing the extrudate surface, the critical pressure for the various samples showing identical $\Delta P_{crit} = 40$ kg/cm^2 reveals some further

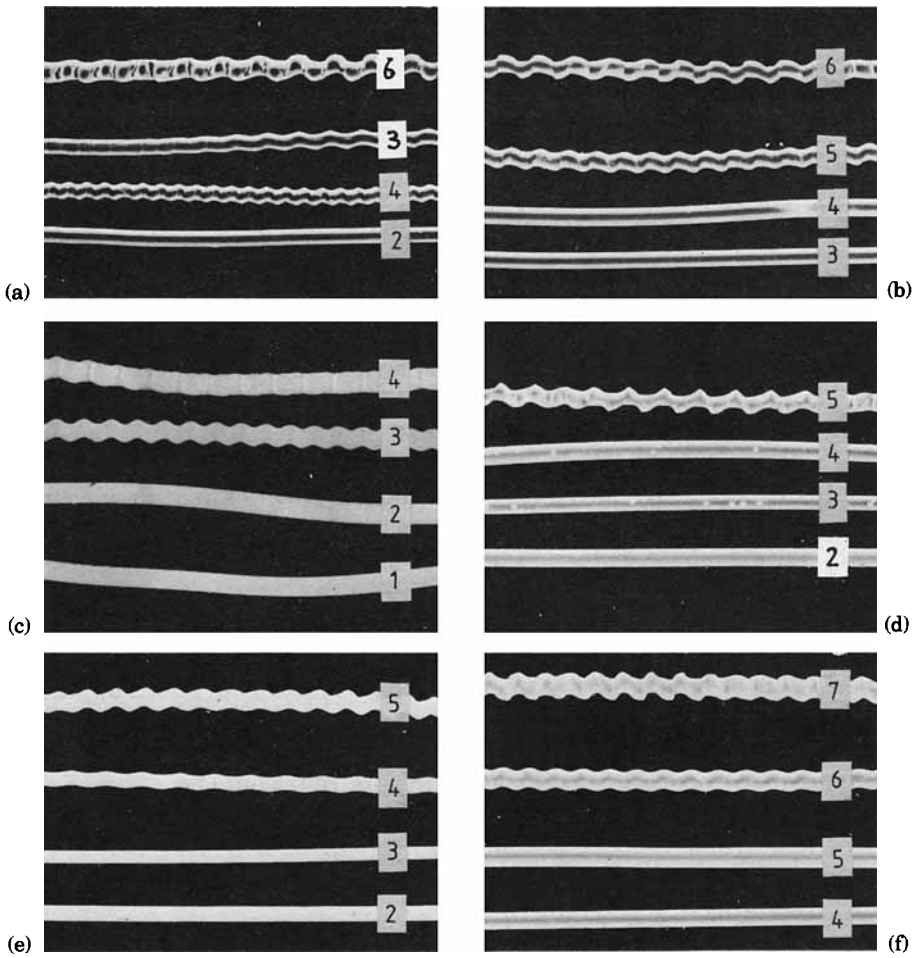

Fig. 6. Photographs of the capillary rheometer extrudates obtained at die L/R ratio = 10, and at various applied pressures ΔP (kg/cm^2): (1) 25; (2) 30; (3) 35; (4) 40; (5) 45; (6) 50; (7) 55; (a) PP; (b) PP/SEBS; (c) PP/PS; (d) PP/HDPE; (e) PP/SEBS/PS; (f) PP/SEBS/HDPE.

distinction in their tendencies for extrudate distortion. Extrudate distortion decreases in the following order:

$$\text{PP/SEBS/PS} > \text{PP/HDPE} \geqslant \text{PP/SEBS} \geqslant \text{PS}$$

Bar diagrams in Figure 7 illustrate distinction of these samples in terms of melt viscosity, melt elasticity, and tendency for extrudate distortion (represented as the reciprocal of ΔP_{crit}). Blends with lower $(\tau_{11} - \tau_{22})$ have higher η_{app}, and their similar profiles of bar diagrams (drawn as broken line curves) indicate a decrease in melt elasticity accompanied by an increase in melt viscosity. However, the extrudate distortion parameter has a somewhat different profile than the linear dependence of tendency for extrudate distortion on melt elasticity and melt viscosity.

These experimentally determined critical shear stresses for extrudate distortion and the variation of melt elasticity with shear stress provide

TABLE V
Values of Various Parameters at Critical Condition of Onset of Extrudate Distortion

Sample	ΔP_{crit} (kg/cm^2)	$(\tau_w)_{crit}$ $\times 10^{-6}$ (dyn/cm^2)	$(\tau_{11} - \tau_{22})_{crit}$ $\times 10^{-6}$ (dyn/cm^2)	$(\eta_{app})_{crit}$ $\times 10^{-3}$ (P)	$(\tau_{11} - \tau_{22})^{1/2}/(\eta_{app})_{crit}$ $\times 10$ [(dyn/cm^2)$^{1/2}$/P]
PP	35	1.71	—	—	—
SEBS	a	—	—	—	—
PS	40	1.96	—	—	—
HDPE	a	—	—	—	—
PP/SEBS	40	1.96	54.2	3.22	2.29
PP/PS	35	1.71	72.1	3.34	2.54
PP/HDPE		1.96	84.4	2.56	3.59
PP/SEBS/PS	40	1.96	28.7	3.92	1.37
PP/SEBS/HDPE	50	2.45	44.1	2.86	2.32

[a] No distortion of extrudate observed in the studied range.

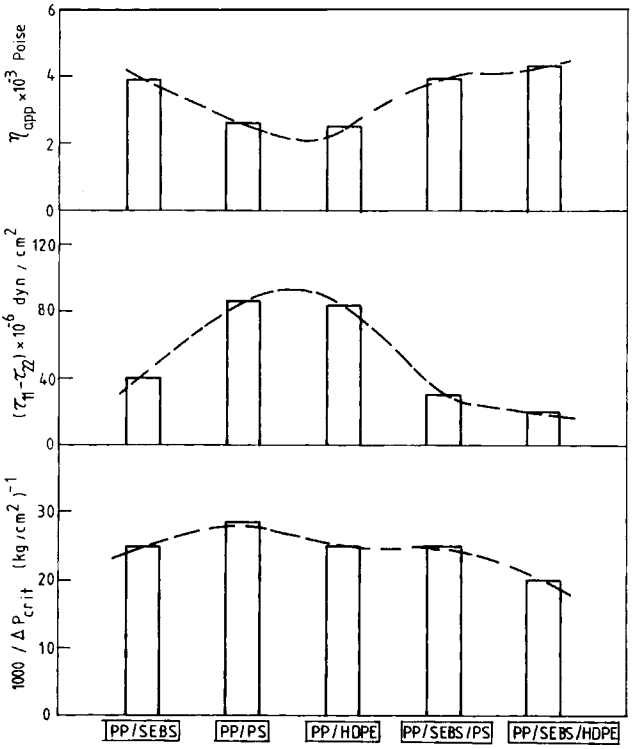

Fig. 7. Bar diagrams showing magnitudes of melt viscosity (η_{app}) and melt elasticity parameter ($\tau_{11} - \tau_{22}$), at shear stress 1.96×10^6 dyn/cm^2, and reciprocal of ΔP_{crit} (a parameter describing the tendency for extrudate distortion).

support to the concept of two-slope character of the melt elasticity parameter vs. shear stress curve suggested in the literature.[22,23] Han and Lemonte[22,23] represented the variation of recoverable shear strain with shear stress with two linear portions with breaking point situated at the critical stress for extrudate distortion. Variations of recoverable shear strain with ΔP (a parameter analogous to shear stress) are shown in Figure 8 for these various samples. The vertical arrows represent the experimentally determined critical values of ΔP shown in Table V for the respective samples. The two-slope character is sufficiently well discernible on these data with breaking points quite consistent with the arrow positions. However, in some cases the two-slope character is not distinct, owing to either large scatter of data points or nonavailability of data in a sufficiently wide range. HDPE shows only one slope, probably owing to no extrudate distortion observed in the range of these measurements.

Dependence of Extrudate Distortion on Material Properties

From the mechanisms of extrudate distortion described by several authors[22–29] and reviewed by Han,[30] it is clear that the higher the exit pressure the higher will be the severity of extrudate distortion. During the flow of a viscoelastic fluid through a capillary, the pressure is highest at the entrance and decays along the length of the capillary depending on the

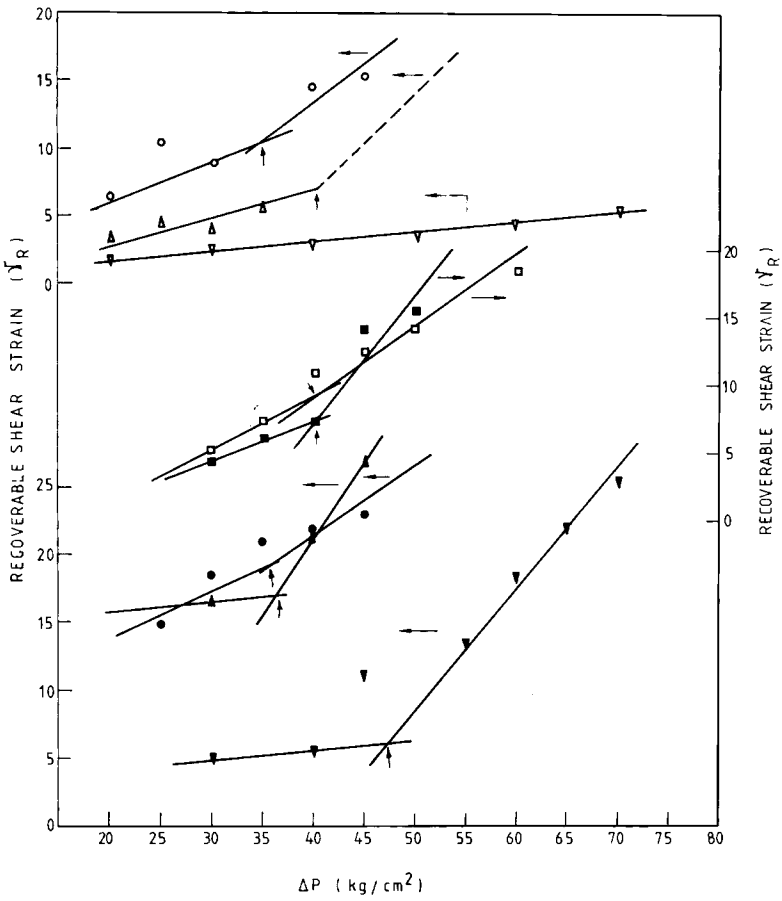

Fig. 8. Variation of recoverable shear strain (γ_R) with ΔP: (○) PP; (△) PS; (▽) HDPE; (□) PP/SEBS; (●) PP/PS; (▲) PP/HDPE; (▼) PP/SEBS/HDPE; (■) PP/SEBS/PS.

properties of the material[14,15,30–35] and finally reaching its lowest value at the exit, called exit pressure P_{exit}. The decay of the pressure amplitude may be treated analogous to the damping characteristics of a viscoelastic material for its dependence on time and elasticity of the material. The decay of pressure amplitude in an element of the fluid flowing from one end of the capillary would thus be greater if its residence time is longer. Or, in other words, the exit pressure will be smaller for longer residence time of the fluid inside the capillary. Owing to inverse proportionality of the volumetric flow rate and the melt viscosity [see eqs. (2) and (3)], the residence time is directly proportional to the melt viscosity. Hence the exit pressure, or the severity of the extrudate distortion (SED), would be inversely proportional to the melt viscosity η_{app}

$$\text{SED} \propto \frac{1}{\eta_{app}} \tag{10}$$

The effect of elasticity on the damping characteristics implies that the greater the elasticity the lower will be the damping. Hence an increase in

melt elasticity should account for an increase in exit pressure or an increase in SED. This may be expressed (for one of the elasticity parameters, viz., $\tau_{11} - \tau_{22}$) as follows, assuming proportionality to the first power:

$$\text{SED} \propto (\tau_{11} - \tau_{22}) \tag{11}$$

It may be stated at this stage that expression (10) is supported by the experimental results[22,23] showing the effect of capillary length on the extrudate distortion, where the severity of extrudate distortion decreased with increasing length of the capillary. The expression (11) has some consistency with the approximate relation $P_{\text{exit}} = (\tau_{11} - \tau_{22})$ stated by some authors[32] or the following more exact relationship[12]:

$$P_{\text{exit}} = (\tau_{11} - \tau_{22}) - \tau_w (dP_{\text{exit}}/d\tau_w) \tag{12}$$

The role of second term on the right-hand side of eq. (12) may be incorporated in expression (11) either through a proper value of constant of proportionality or through the use of a suitable exponent n; using the latter alternative leads to following form of expression (11):

$$\text{SED} \propto (\tau_{11} - \tau_{22})^n \tag{13}$$

Combining expressions (10) and (13) yields

$$\text{SED} \propto \frac{(\tau_{11} - \tau_{22})^n}{\eta_{\text{app}}} \tag{14}$$

Values of melt viscosity and melt elasticity at the critical shear stress for these blend samples show sufficiently linear variation of $\log(\tau_{11} - \tau_{22})$ vs. $\log \eta_{\text{app}}$, shown in Figure 9, suggesting a relationship of the following form:

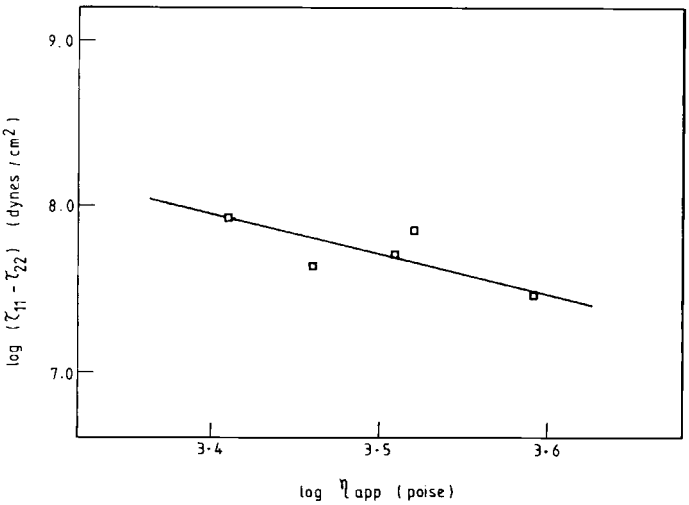

Fig. 9. Variation of $\log(\tau_{11} - \tau_{22})$ vs. $\log \eta_{\text{app}}$.

$$\eta_{app} = K'(\tau_{11} - \tau_{22})^{0.5} \quad (15)$$

where K' is a constant. This suggests a constant value of $(\tau_{11} - \tau_{22})^{0.5}/\eta_{app}$ at the critical shear stress, and thus a possible value 0.5 for the exponent n in expression (14).

Thus it may be stated that the critical limit, for the extrudate distortion to become observable, is reached when the value of the ratio $(\tau_{11} - \tau_{22})^{1/2}/\eta_{app}$ surpasses a critical value. Values of $(\tau_{11} - \tau_{22})^{1/2}/\eta_{app}$ at the critical stress for these blends, shown in Table V, are quite close to a critical value of this ratio described by the mean value, viz., 2.42 ± 0.79. The observed deviation of these data around the mean value may be associated with the wide step of variation of ΔP used in these measurements (i.e., $\pm$ 5 kg/cm^2). A smaller deviation might be expected if the measurements were done using finer steps of variation of ΔP. Further work would be useful to ascertain this relationship of melt elasticity and melt viscosity with the extrudate distortion behavior. Furthermore, there is a scope of incorporating any other property or parameter through a constant of proportionality in expression (14).

State of Dispersion

In all these blends, PP, being the major component, forms a continuous phase, while the other components PS, HDPE, and SEBS form discrete phases, as expected from the known mutual immiscibility of all these components. The discrete phase character of all these components in PP matrix is also shown from the scanning electron micrographs of cryogenically fractured surfaces of compression-molded sheets shown in Figure 10 and of extrudates shown in Figure 11 of these blends. The samples were etched in xylene at room temperature to dissolve out the PS and SEBS phases, which leave empty spaces of their characteristic shapes appearing black in these micrographs. Domains of PS in PP/SEBS/PS blend are clearly distinguishable from a comparison of the two samples containing PS, viz., PP/PS [Fig. 10 (a)] and PP/SEBS/PS [Fig. 10(b)]. The PS domains are small and round in shape while the SEBS domains are larger and of irregular shapes. The rounded shape of PS domains in PP matrix, also observed by other authors,[31] is indicative of greater nonaffinity of PS with PP than of SEBS with PP. The polyolefinic block EB of SEBS as well as HDPE might be expected to have some affinity with the PP matrix phase, which might account for their lower tendency of forming round or spherical domains. Identification of HDPE domains is not so distinct, owing to the limitations of the etching procedure used.

However, some regions of HDPE terminating at the PP matrix through fibrillar endings are apparent on the micrographs of the compression-molded sample [Fig. 10(d)] and formation of a somewhat distinct network structure of HDPE phase is seen in the micrograph of extrudate sample of PP/SEBS/HDPE blend (Fig. 11).

In case of extrudate samples, though the micrographs (Fig. 11) correspond to the transversely fractured surface, some longitudinal regions are also apparent due to the irregularities of the fracture surface. The major portions of these micrographs represent the transverse surface (perpendicular to the

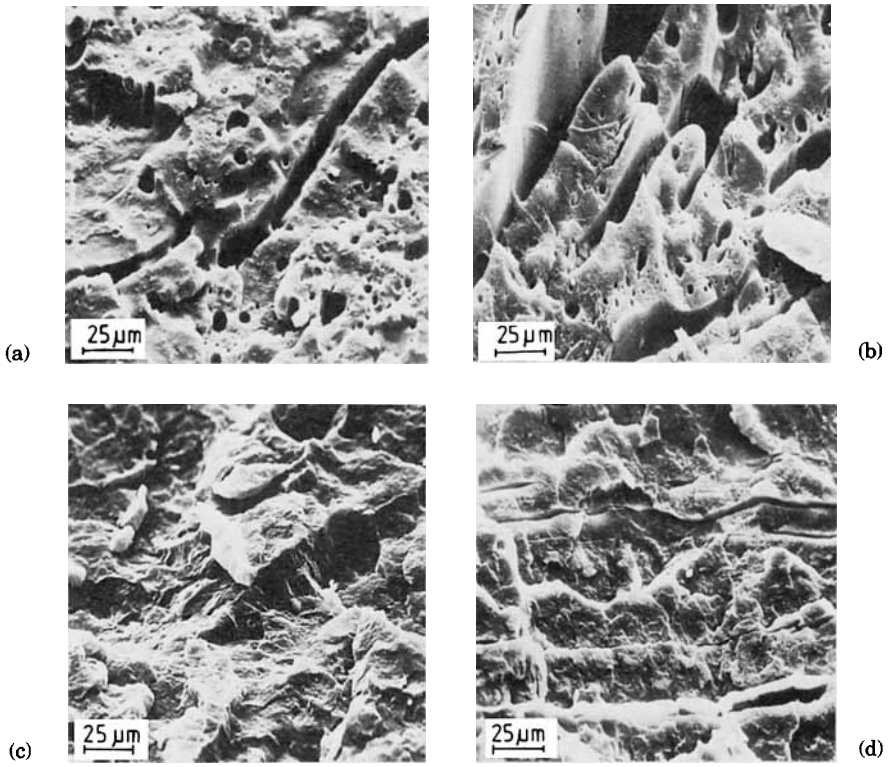

Fig. 10. Scanning electron micrographs of cryogenically fractured surfaces of compression moulded sheets, etched with xylene: (a) PP/PS; (b) PP/SEBS/PS; (c) PP/SEBS; (d) PP/SEBS/HDPE.

direction of flow) where discrete phase domains are the cross sections of the domains elongated in the direction of flow or shear stress. Elongation of SEBS domains along the flow direction was observed earlier also.[1] Appearance of sufficiently sharp lines in the longitudinal section portions on these micrographs of PP/PS (Fig. 11) shows the elongation of PS domains along the flow direction. Also apparent in these micrographs is the size difference between the PS and SEBS domains; SEBS domains are much larger than PS domains in these blends of identical blending ratios. A considerable tendency of locallization of SEBS domains in PP matrix at similar blending ratios was observed earlier also.[1] Formation of vortex or any preferential alignment of discrete phase domains towards the axis or the wall of the capillary, observed for some blends by Han and Yu,[31] is not seen in these blends as apparent from the micrographs of the entire area of these extrudate surfaces in Figure 12.

These scanning electron micrographs show no major morphological changes, such as the mutual association of the two discrete phases or any significant agglomeration of domains of the same phase, during flow through capillary; state of dispersion before and after the flow is represented by the compression-molded and the extrudate samples, respectively.

Melt rheological properties of the blends depend not only on the morphology of its components, but also on viscosities of the components and

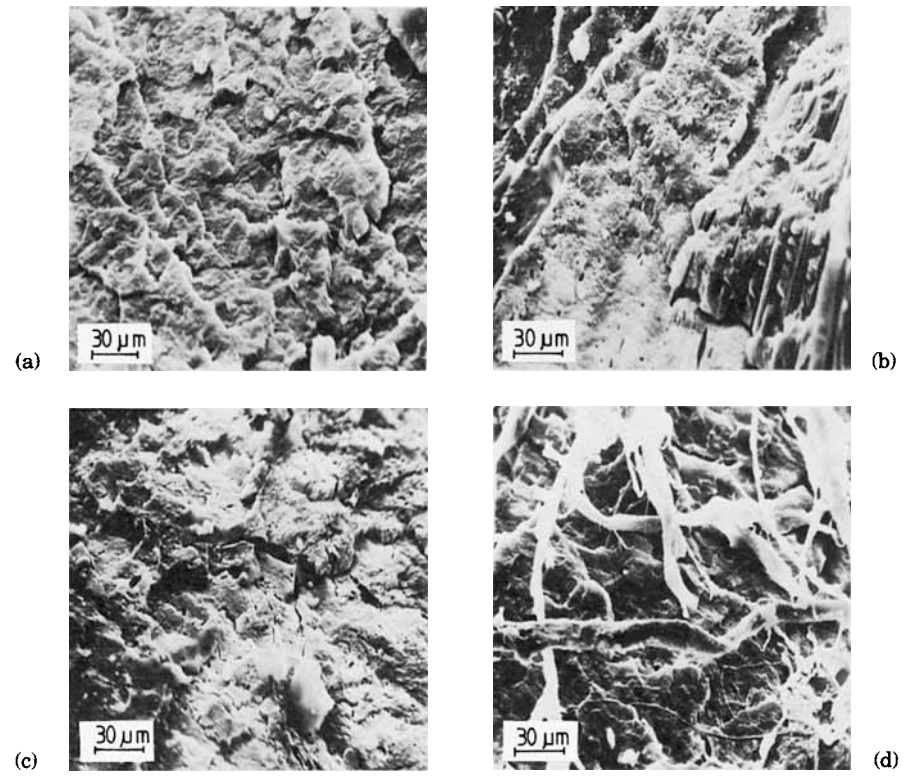

(a) (b) (c) (d)

Fig. 11. Scanning electron micrographs of cryogenically fractured surfaces of capillary rheometer extrudates obtained at shear stress 1.96×10^6 dyn/cm^2, etched with xylene: (a) PP; (b) PP/PS; (c) PP/SEBS/PS; (d) PP/SEBS/HDPE.

their mutual interactions, etc. Though the exact mechanisms are not easy to ascertain, some comments possible from these data are given below.

Owing to their considerably higher viscosities than the matrix phase, the discrete phase domains may be treated as the case of rigid suspensions in a fluid of low viscosity. Resistance to flow would increase with increasing size and decreasing flexibility of the dispersed domains. The observed higher viscosity of the PP/SEBS blend than the PP/PS blend is in agreement with this view. Viscosity of the blend showing network morphology, viz., the PP/HDPE, is quite comparable to that of PP/PS. Though the network structure produces greater resistance to flow, the effects of cohesive forces of each phase may alter this effect.[34]

These ternary blends may be treated as the two kinds of suspensions present in the same fluid. The SEBS domains, which are sufficiently larger in size, seem to play a predominant role in the melt flow properties of these ternary blends. Melt viscosities of both the ternary blends, PP/SEBS/PS and PP/SEBS/HDPE, are higher than the corresponding binary blends (without SEBS component) and quite comparable to the PP/SEBS blend.

The role of SEBS in decreasing melt elasticity seems attributable to the elastomeric nature of this component, which in its molten state is capable of absorbing greater energy of deformation with smaller elastic recovery. The ternary blends show lower melt elasticity than the binary blend con-

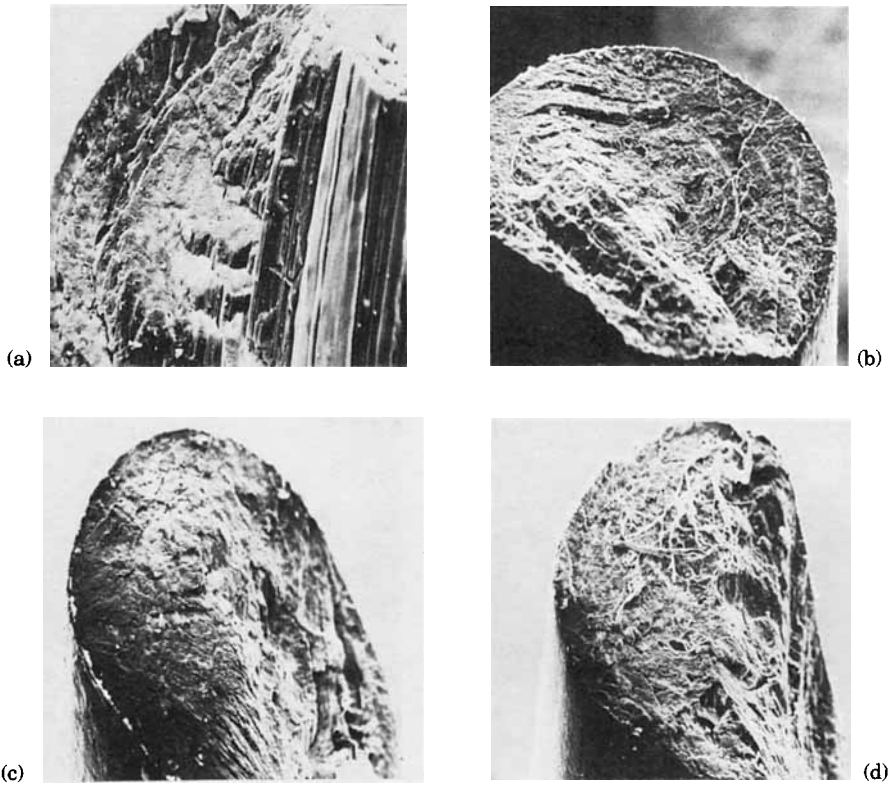

Fig. 12. Scanning electron micrographs of cryogenically fractured surfaces of capillary rheometer extrudates obtained at shear stress 1.96×10^6 dyn/cm^2 etched with xylene, at a lower magnification showing the entire surface area: (a) PP/PS; (b) PP/SEBS; (c) PP/SEBS/PS; (d) PP/SEBS/HDPE.

taining SEBS (i.e., PP/SEBS), in spite of a much higher melt elasticity of their corresponding binary blends (i.e., PP/PS and PP/HDPE). Probably a part of the elastic recovery stresses of the SEBS domains are shared or absorbed by the PS or HDPE phases and thus result in smaller overall elastic recovery of the blend.

CONCLUSION

Although the advantages of blending with SEBS in improving various properties of PP are known from the previous works,[1-3] this study reveals the scope of further improvements of properties by incorporation of a suitable third component in PP/SEBS blend. Also revealed from this study is the effect of addition of SEBS to PP/PS and PP/HDPE blends. The present choice of blend composition, for binary blends PP/X and ternary blends PP/X/Y, enabled us to see the effect of 10 wt % addition of X to PP, Y to PP/X blend of 90:10 composition, or X to PP/Y blend of 90:10 composition, where X and Y are either of the following three: PS, HDPE, and SEBS.

Improvements in processability of PP on blending with these one or two components are seen in the lowering of softening and flow temperatures. Melt viscosity of the binary and the ternary blends containing SEBS (viz.,

PP/SEBS, PP/SEBS/PS, and PP/SEBS/HDPE) was higher than the other blends (viz., PP/PS and PP/HDPE). Melt elasticity, on the other hand, was lower for the ternary blends (viz., PP/SEBS/PS and PP/SEBS/HDPE) than the binary blends containing SEBS (viz., PP/PS and PP/HDPE). Among the three binary blends, PP/PS and PP/HDPE had considerably higher melt elasticity than the PP/SEBS.

Tendency for extrudate distortion differed in these different blends, and was lowest for the PP/SEBS/HDPE blend and highest for the PP/PS blend and the unblended PP. A model for the effect of material properties, viz., melt viscosity and melt elasticity, on the severity of extrudate distortion at the critical shear stress (i.e., where it reaches the limit of its first appearance) is presented, along with its experimental support from these data. According to this, the critical stage for first appearance of the distortion of extrudate surface reaches when $(\tau_{11} - \tau_{22})^{1/2}/\eta_{app}$ reaches a critical value.

Scanning electron microscopy showed discrete two-phase (for binary blends) and three-phase (for ternary blends) morphology of all these blends; the discrete phase character remained unchanged during flow through the capillary. Viscosities, elasticities, shapes, sizes, and deformabilities of the discrete phase domains accounted sufficiently well for the observed differences in the melt rheological parameters of these different blends.

References

1. A. K. Gupta and S. N. Purwar, *J. Appl. Polym. Sci.* **29**, 1079 (1984).
2. A. K. Gupta and S. N. Purwar, *J. Appl. Polym. Sci.* **29**, 1595 (1984).
3. A. K. Gupta and S. N. Purwar, *J. Appl. Polym. Sci.*, **29**, 3513 (1984).
4. C. R. Lindsey, D. R. Paul, and J. W. Barlow, *J. Appl. Polym. Sci.*, **26**, 1 (1981).
5. T. D. Traugott, J. W. Barlow, and D. R. Paul, *J. Appl. Polym. Sci.*, **28**, 2947 (1983).
6. D. L. Siegfried, D. A. Thomas, and L. H. Sperling, *J. Appl. Polym. Sci.*, **26**, 177 (1981).
7. D. E. Zurawski and L. H. Sperling, *Polym. Eng. Sci.*, **23**, 510 (1983).
8. A. F. Yee and J. Diamant, *Am. Chem. Soc., Polym. Prepr.*, **19**, 92 (1978).
9. P. Kratochvil, private communication, 1984.
10. T. Arai, *A Guide to Testing of Rheological Properties of Polymers by Koka Flow Tester*, Maruzen, Tokyo, 1958.
11. A. K. Gupta, V. B. Gupta, R. H. Peters, W. G. Harland, and J. P. Berry, *J. Appl. Polym. Sci.*, **27**, 4669 (1982).
12. C. D. Han, *Rheology in Polymer Processing*, Academic, New York, 1976, Chap. 5.
13. R. S. Lenk, *Polymer Rheology*, Applied Science, London, 1978, Chap. 1.
14. C. D. Han, T. C. Yu, and K. U. Kim, *J. Appl. Polym. Sci.*, **15**, 1149 (1971).
15. C. D. Han, *J. Appl. Polym. Sci.*, **15**, 2591 (1971).
16. L. A. Utracki, *Polym. Eng. Sci.*, **23**, 602 (1983).
17. O. Truesdell, *Trans. Soc. Rheol.*, **4**, 9 (1960).
18. S. L. Green, S. Middleman, and J. Gavis, *J. Appl. Polym. Sci.*, **3**, 367 (1960).
19. S. Middleman and J. Gavis, *Phys. Fluids*, **4**, 355 (1961).
20. J. Gavis and S. Middleman, *J. Appl. Polym. Sci.*, **7**, 493 (1963).
21. R. I. Tanner, *J. Polym. Sci. A-2*, **8**, 2067 (1970).
22. C. D. Han and R. R. Lamonte, *Polym. Eng. Sci.*, **11**, 385 (1971).
23. C. D. Han and R. R. Lamonte, *Polym. Eng. Sci.*, **12**, 77 (1972).
24. R. S. Spencer and R. E. Dillon, *J. Colloid Sci.*, **4**, 241 (1949).
25. J. P. Tordella, *J. Appl. Phys.*, **27**, 454 (1956).
26. J. P. Tordella, *Trans. Soc. Rheol.*, **1**, 203 (1957).
27. J. P. Tordella, *Rheol. Acta*, **1**, 216 (1958).
28. E. B. Bagley, *Trans. Soc. Rheol.*, **5**, 355 (1961).
29. E. B. Bagley and H. P. Schreiber, *Trans. Soc. Rheol.*, **5**, 341 (1961).

30. C. D. Han, *Rheology in Polymer Processing*, Academic, New York, 1976, Chap. 12.
31. C. D. Han and T. C. Yu, *J. Appl. Polym. Sci.*, **15**, 1163 (1971).
32. C. D. Han, *J. Appl. Polym. Sci.*, **15**, 2567 (1971).
33. C. D. Han, *J. Appl. Polym. Sci.*, **15**, 2579 (1971).
34. B. Maxwell and G. L. Jasso, *Polym. Eng. Sci.*, **23**, 614 (1983).

Received April 27, 1984
Accepted July 19, 1984